Chapter 1

Pollutant Degradation in Gas Streams by means of Non-Thermal Plasmas

Milko Schiorlin, Cristina Paradisi,
Ronny Brandenburg, Michael Schmidt,
Ester Marotta, Agata Giardina and Ralf Basner

Additional information is available at the end of the chapter

http://dx.doi.org/10.5772/60049

1. Introduction

In the industrialized society air pollution has become a major concern for the environment and public health. Pollutants such as particulate matter and harmful chemicals are causing disease or death to humans and other living organisms and strongly affect ecosystems (e.g. acidification, eutrophication). Although significant progress has been made in recent years in tackling the emissions of some air pollutants (e.g. sulphur dioxide), a large fraction of the population is still exposed to excessive concentrations of certain air pollutants, in particular volatile organic compounds, particulate matter, and ammonia. Therefore, environmental standards are continuously being raised and more effective technologies for depollution of gas streams are needed.

Air non-thermal plasmas (NTPs) are strongly oxidizing environments and thus useful means for the activation of advanced oxidation processes for air and water remediation. NTPs are used for the generation of ozone as an important oxidant for water or air cleaning and the removal of dust from flue gases in electrostatic precipitators [1, 2, 3]. Within the last years deodorization by means of NTP or NTP-supported methods has reached the level of commercialisation.

The term plasma denotes an ionised gas containing free electrons, ions and neutral species (atoms and molecules) characterized by collective behaviour. Often referred to as the "4th state of matter", plasmas have unique physical and chemical properties distinct from solids, liquids and gases. They are electrically conductive, respond to electromagnetic fields, contain chemically reactive species as well as excited species and emit electromagnetic radiation in

various wavelength regions. Plasmas are generated artificially by supplying energy to gases, liquids or solids.

In principle, gaseous plasma depollution can be done by an increase of the gas enthalpy in so-called "translational" plasmas, which are non-equilibrium plasmas (electrons and heavy particles have different mean kinetic energies) but with gas temperatures reaching several thousand K. Plasma torches, arcs, arc jets or gliding arcs are examples for such plasma-based incineration sources [4]. However in the following we will focus on non-thermal plasmas which stays at moderate gas temperatures, also referred to as "cold" non-thermal plasmas. Another approach, which is also excluded in this chapter, is the electron beam injection, which is under development for very large combustion facilities (coal fired power plants) [5].

The most common method of producing "cold" non-thermal plasmas for technological applications is based on the application of an electric field to a gas. If the applied field exceeds a certain threshold value (breakdown field strength) a gas discharge and thus plasma are generated. The specific feature of so-called non-thermal plasmas is that most of the coupled energy is primarily released to the free electrons which exceed in temperature that of the heavy plasma components (ions, neutrals) by orders of magnitude. Thus, strong non-equilibrium conditions are achieved in which the gas temperature remains nearly at or slightly above room temperature ("cold") while "hot" electrons initiate chemical processes resulting eventually in the oxidation of pollutants.

This chapter is meant to provide some insight into the application of NTP for air remediation. After a brief introduction to summarize the principles of NTP generation, the main aspects of discharge physics and plasma chemistry involved in air treatment are described and discussed. Special focus is on the removal of volatile organic compounds (VOCs). The two major types of plasma sources for such applications, namely dielectric barrier discharges and corona discharges, are described in the next section. Various aspects of plasma generation and the ensuing chemical processes will be discussed in two separate sections based largely on work carried out by the Authors in Padova and in Greifswald. Finally, some conclusions and perspective outlook on the field are given.

2. Overview non-thermal plasma-reactors and processes for depollution of gases

The most common principles for the generation of "cold" non-thermal plasmas are dielectric barrier discharges (DBDs) and corona discharges. They are most suitable for treating exhaust gases from manufacturing processes and mobile emission sources, as they offer a compact design and good scalability.

DBD based devices consist of at least two electrodes enclosing a gas space which is filled with, or bound by, an insulating material [6]. Typically, dielectric materials such as glass, quartz, ceramics, enamel, plastics, silicon rubber or Teflon are used as barrier materials. There are many possible DBD arrangements. Traditionally, DBDs were generated in parallel plate reactor

http://dx.doi.org/10.5772/60049

geometries or in coaxial cylindrical reactor geometries, as shown in Figure 1 (left). The dielectric barrier(s) can cover one or both electrodes entirely, but they can also be separated from both electrodes, forming two discharge gaps. The gap widths are typically in the range of 0.1 – 5 mm. When a sufficiently high voltage is applied between the electrodes, an electrical breakdown occurs and plasma is formed. Furthermore, both electrodes can be arranged in such a way that they are in direct contact with the barrier. In this case, the gas discharge is formed in the gas at the exposed electrode and propagates along the dielectric surface, and is therefore called 'surface discharge' or 'surface DBD'. In 'co-planar DBDs' both electrodes are embedded in the insulator. The so-called 'sliding DBD' is based on surface DBDs but with a third electrode which is placed opposite to the top electrode on the dielectric surface [7]. This arrangement allows the discharge 'to slide' over the dielectric. The so-called 'packed bed reactor' is also often classified as DBD-type plasma. Dielectric or ferroelectric pellets are packed in between the two electrodes. Due to polarization of the pellet material, regions with high electrical fields are generated, leading to gas discharges in the void spaces between the pellets and on their surfaces [8]. Porous ceramic foams can also be used instead of pellets beds [9]. Packed-bed reactors are relevant for depollution since the filling can feature catalytic properties.

The insulator suppresses large currents on the electrodes and thus keeps the plasma in the non-thermal regime [6]. Because of the capacitive coupling of the insulating material to the gas gap, DBD generation requires alternating or pulsed operating voltages. For the treatment of gas streams the gas is injected into the device flowing along the electrode arrangement. In industry DBDs are used for the generation of ozone, deodorization, surface treatment and many more.

Corona discharges are characterized by non-uniform electrical field geometries, e.g. needle-to-plate or wire-in-cylinder electrode arrangements, as shown in Figure 1 (right). DC and low frequency AC operated corona discharges expand from the needle or wire electrode in the outer regions towards the plate or cylinder electrode. The energy is mainly dissipated in the high-ohmic region of non-ionized gas in the outer drift region, where the electrical field is lower than in the plasma region around the wire/needle electrode. In this region the discharge is not supported anymore and is thus kept in the non-thermal regime [10]. DC-operated corona discharges are used in electrostatic precipitators. For environmental applications (e.g. VOC removal, water purification) corona discharges operated by pulsed high voltage are proposed since higher densities of reactive species can be achieved [11]. Pulsed corona discharges are characterized by plasma regions which fill a much larger fraction of the discharge gap than DC or low frequency corona discharges.

In molecular gases at atmospheric pressure, corona discharges and DBDs are typical examples of non-uniform, filamentary plasmas, consisting of many individual microdischarges or discharge channels. Each volume element of the flowing gas is repeatedly subjected to the action of these filaments as it passes through the reactor. Non-thermal plasma based remediation of air is due to chemical reactions with photons and active species created in the plasma, namely radicals or ions. The different physical and chemical processes associated with and induced by non-thermalizing discharges span a time range of about 12 orders of magnitude. The equilibrium of the electrons with the local electrical field is usually approached within

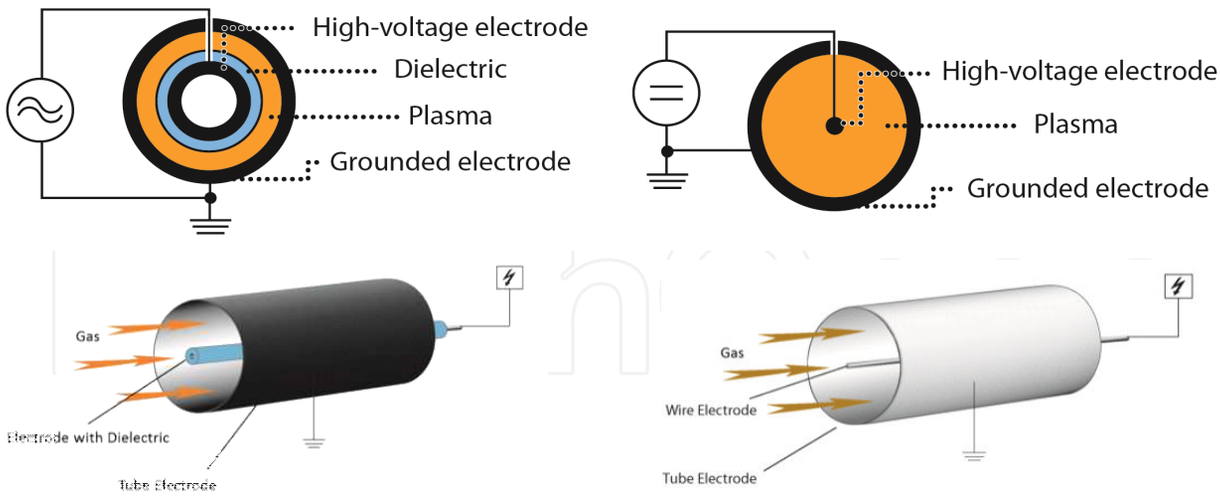

Figure 1. Top pictures: Cross sectional view of coaxial DBD (left) and DC corona discharge (right) arrangement; Bottom pictures: Coaxial DBD (left) and corona discharge (right) reactor for treatment of air streams.

picoseconds [6, 12, 13]. Ionization and electrical breakdown typically proceed at the nanosecond time scale via electron collisions. For example, DBD microdischarges in atmospheric air have duration of about 20 - 50 ns. The development of discharge channels and microdischarges is dominated by the build-up and spatio-temporal enhancement of volume space charges, resulting in propagating perturbation of the electric field, which has been investigated as a cathode directed streamer or ionization wave [12, 13]. In the filaments the highest electron density and electron temperature are achieved and electron-induced dissociation and thus formation of radicals occur. The pollutant degradation is initiated by secondary reactions with these free radicals and ions, mainly on a micro- to millisecond time scale, i.e. after the active discharge filament has faded [14]. Ion-molecule reactions occur on an intermediate time scale, typically in the range of 10 ns up to 1 μs. The pollutant molecules react with oxidizing atoms and radicals (e.g. O, OH) or with plasma-generated ozone (O_3). Water vapor may play an important role, as it acts as the precursor for hydroxyl radicals (OH) and hydroperoxyl radicals (HO_2). When hydrocarbons or other VOCs are present in the gas, other radicals are also produced and radical chain reactions occur. Beside electrons, photons or collisions with metastable or excited species can lead to ionization.

The chemical equilibrium including heat and mass transfer is commonly settled within milliseconds to seconds.

The application of NTP for pollutant degradation in gases in industry must comply with the demands on removal efficiency, energy efficiency and selectivity.

The removal efficiency is defined as the removed molar fraction of the pollutant related to the initial molar fraction C_{in}: $\eta=(C_{in}-C_{out})/C_{in}$ (C_{out} is the molar fraction of the pollutant after the plasma treatment) [2, 14]. Energy efficiency relates to the energy needed to achieve a given removal efficiency and can be expressed in several ways. For example the energy yield is the decomposed pollutant mass per dissipated energy. A high energy yield is not necessarily

assuring sufficient removal efficiency as this is determined by the initial molar fractions of the pollutant [2]. The removal efficiency and the energy efficiency depend on the specific energy density of the plasma and are also determined by a number of conditions (gas composition, humidity and temperature; level of initial contamination) [2, 14].

Selectivity is defined as the fraction of the desired product of the plasma-chemical conversion to the total amount of products of the conversion process. The chemistry and fraction of desired products and undesired by-products can also be characterized by mass balances (e.g. carbon balance in the case of conversion of hydrocarbons). A high selectivity is required to achieve a reasonable performance in terms of energy efficiency and by-products [2]. High reactivity of radicals usually results in a poor selectivity, since competing reactions which result in the formation of undesired by-products happen simultaneously. One important reaction which consumes oxygen atoms alongside the reactions with pollutant molecules is the generation of O_3. For some pollutants (e.g. $NO_{x,}$ alkenes and other unsaturated VOCs) O_3 is an efficient oxidizer, but in other cases it constitutes an additional pollutant by-product.

In the following paragraphs the main aspects of pollutant degradation by means of DBDs and corona discharges are discussed using selected examples. The discussion is focussed on VOCs as a class of contaminants present in many different industries (e.g. semiconductor manufacturing, chemical processing, painting and coating) as well as in indoor air (outgassing of paint, carpets etc.). VOCs contribute to the generation of photochemical smog and to certain health diseases like nausea and skin irritation. Some are associated with high cancer risk [15, 16]. Conventional methods for VOCs removal are thermal oxidation, condensation, absorption and biofiltration. The thermal oxidation and condensation are economic only for situations in which VOCs are present in moderate to high concentrations. The absorption process does not destroy VOCs but only transfers them to another medium. In addition, this technology suffers from problems arising by deposits of dirt or clog on filters. Biofilters are useful only for VOCs that have some solubility in water and they are cost-effective if the volume of air to be treated is in the range of $10^4 – 10^5$ m^3/h. In NTP energy of about 10-30 eV are needed to produce an O-atom or an OH-radical in (humid) air, which makes the decomposition also energy consuming [14]. However, the total energy consumption can be low in case of small concentrations of pollutants. Thus NTP-based processes are feasible for low contamination levels. For VOCs, this level is about 100 mg/m_N^3 (N refers to standard conditions for pressure and temperature) [2, 14].

Among the different VOCs which are being routinely monitored for air quality, toluene (methylbenzene, C_7H_8) is one of the most important ones. Toluene is widely used as feedstock in the chemical industry for the synthesis, among others, of drugs, dyes, explosives, and as a solvent (e.g. thinner, paints, adhesives). Exposure to toluene is known to affect the central nervous system and may cause tiredness, confusion, weakness, memory loss, and nausea. Toluene is water-insoluble and thus cannot be scrubbed. For its wide use, diffusion and well known properties and reactivity, toluene has become sort of a standard for testing and comparing non-thermal plasma based air treatment for VOCs removal. Thus, the discussion in the following sections will focus largely on experiments with toluene. The conversion of toluene in hybrid systems in which NTP is combined with a catalyst is also being extensively studied and has been reviewed [17]. Such hybrid processes will not be covered in this chapter.

3. VOC removal by means of corona discharges

Air plasma produced by corona discharges and its performance in the oxidation of VOCs are being investigated in Padova using a prototypal large corona reactor [18–20]. The reactor and the auxiliary apparatus were designed in order to achieve stable and reproducible plasma regimes and experimental conditions, which are necessary for quantitative kinetic and product studies. Reproducibility and stability of experimental conditions in our set-up allow to test and compare the performance of different corona regimes, notably dc+, dc– and pulsed+ within the same apparatus and under otherwise identical experimental conditions. The experimental set-up, comprising the corona reactor, the gas flow line and instrumentation for *in line* and *off line* analysis of the treated gas, is schematically reproduced in Figure 2.

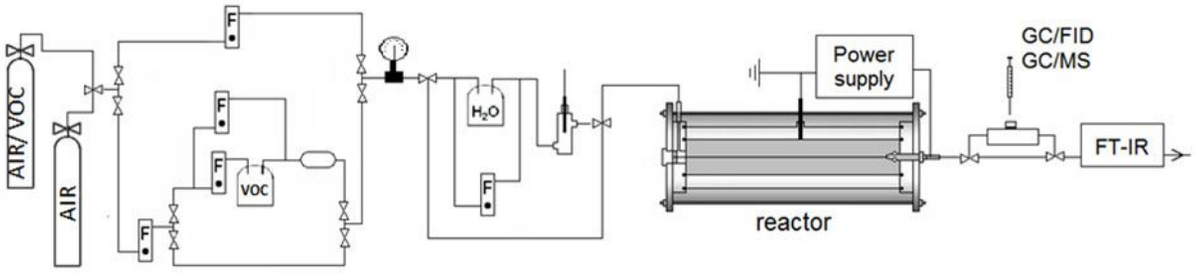

Figure 2. Schematics of corona reactor, gas flow line and instrumentation for *in line* and *off line* analysis of the treated gas.

The corona reactor has a wire/cylinder electrode configuration. The wire electrode (stainless steel, outer diameter 1 mm) is electrically connected to the high voltage supply and fixed along the axis of a stainless steel cylinder (38.5 mm i.d. x 600 mm) which is electrically grounded.

The reactor can be energized by dc or pulsed high-voltage power. The dc power supply has an output voltage of ± 25 kV and an output current of 0 – 5 mA. For generating pulsed corona, a pulsed high voltage with dc bias (PHVDC) was used, based on a spark gap switch with air blowing, with the following specifications: dc bias of 0 – 14 kV, peak voltage of 25 – 35 kV (with dc bias), peak current up to 100 A, maximum frequency 300 Hz, rise-time of the pulses less than 50 ns. To measure the power input two homemade current probes (*shunt*), one of 1.1 Ω for pulsed current, the other of 52 Ω for dc current, were used. The experimental apparatus was described in detail previously [18].

The reactor is connected to a gas flow line made of Teflon tubing (inner diameter 4 mm). The air/VOC mixture is prepared by bubbling synthetic air (80% nitrogen: 20% oxygen from AirLiquide) through a sample of liquid VOC and by diluting the outcoming flow with a second flow of synthetic air to achieve the desired gas composition (VOC mixing ratio in the 100 - 1000 ppm range) and flow rate (usually kept constant at 450 $mL_N \cdot min^{-1}$). The gas flow line is equipped with a loop for humidification and with a probe to measure the humidity. The treated gas exiting the reactor goes through a small glass reservoir equipped with a sampling port from which aliquots are withdrawn with a gastight syringe for off-line chemical analysis by

http://dx.doi.org/10.5772/60049

GC-MS (Agilent Technologies 5973) and GC-TCD/FID (Agilent Technologies 7890). *In line* IR analysis is performed with an FTIR Nicolet 5700 spectrophotometer using a 10 cm long gas cell with windows of NaCl (for experiments with dry air) or of CaF_2 (for experiments with humidified air). The determination of ozone, CO, and CO_2 were performed by integration of characteristic IR bands as described previously [18]. The determined conversion data, i.e. $[VOC]/[VOC]_0$ as a function of the specific input energy (SIE, also referred to as specific energy density SED) usually follow a first order exponential decay profile. The SIE was determined as described previously for dc [18, 21] and pulsed [20, 21] corona, respectively. The data are thus interpolated with the equation (1) to obtain the energy constant kE, which is a measure of the process energy efficiency.

$$[VOC] = [VOC]_0 \cdot e^{(-k_E \cdot SIE)} \tag{1}$$

Current/voltage characteristics of dc corona, both of positive and negative polarity, were monitored in synthetic air with and without VOC admixture (500 ppm VOC concentration). For each applied voltage, the mean current intensity was measured, after a stabilization time of 5 minutes, using a multimeter. The ions present in the air plasma produced by +dc and –dc corona were investigated using an APCI (*Atmospheric Pressure Chemical Ionization*) interfaced to a quadrupole mass analyzer (TRIO 1000 II, Fisons Instruments) [22, 23]. A schematic drawing of the arrangement and the gas inlet systems is shown in Figure 3.

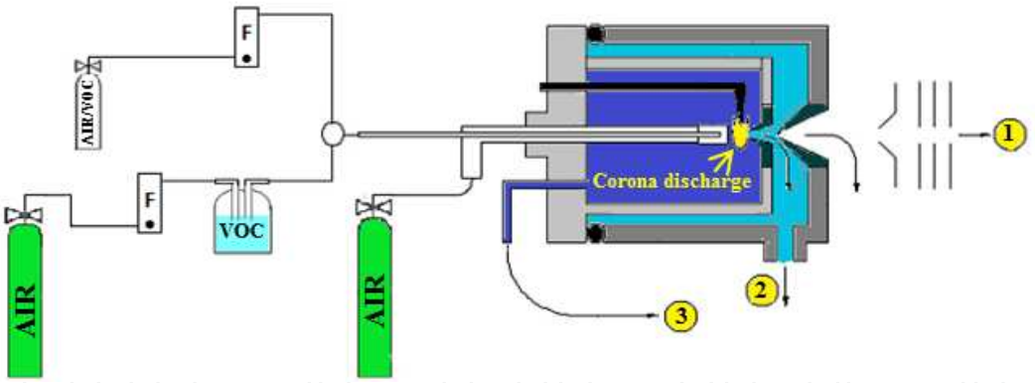

Figure 3. Schematics of APCI ion source and gas inlet system (1) quadrupole analyzer, (2) rotary pump, (3) diaphragm pump.

The corona discharge is kept at atmospheric pressure by a flow of synthetic air (4–5 $L \cdot min^{-1}$) introduced through the nebulizer line, a capillary of ca. 2 mm (inner diameter). Vapors of the desired VOC, stripped by an auxiliary flow of synthetic air (typically 5–50 $mL \cdot min^{-1}$) from a liquid sample contained in a reservoir, enter the APCI source through another capillary (inner diameter 0.3 mm) placed coaxially inside the nebulizer line. A second line allows for the introduction of water vapors as desired. The needle electrode for corona discharge was kept at 3 kV. Ions leave the source through an orifice (50 μm in diameter) in the counter electrode, called the "sampling cone" and held at 0–150 V relative to ground. The ions then cross a low

pressure region (down to ca. 10^{-2} Torr) and, through the orifice in a second conical electrode, called the "skimmer cone" and kept at ground potential, reach the low pressure region hosting the focusing lenses and the quadrupole analyser. Prior to running the experiments with the VOC, a preliminary analysis is routinely conducted to acquire the "background" spectra with only synthetic air and humidified synthetic air [a)].

The efficiency, products and mechanisms of VOC oxidation were studied systematically under variation of the corona type (dc or pulsed), the corona polarity (negative or positive), the VOC (a few hydrocarbons, halogenated and oxygenated organic compounds have been investigated), the VOC inlet concentration and the level of humidity. These studies have provided a large body of experimental results which give insights into corona induced chemical oxidation and useful hints for its application.

The type of corona has major impact on the process efficiency. In Figure 4 an example is shown, which is reporting a comparison of the decay profile of toluene concentration as a function of SIE under three different corona regimes: dc+, dc– and pulsed+ [21]. The much better efficiency of pulsed+ corona with respect to dc corona of either polarity is evident. Also evident is the better performance of dc– with respect to dc+ corona. Analogous results were obtained in similar experiments with other VOCs, including *n*-hexane [18, 20] and dibromomethane [24].

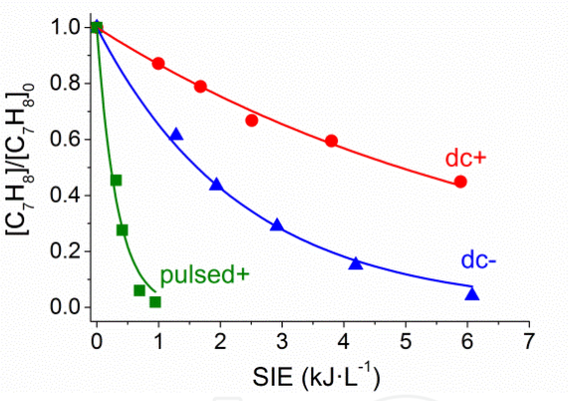

Figure 4. Decay profile of toluene (500 ppm in synthetic air) as a function of SIE in corona induced oxidation under the following regimes: pulsed+, dc– and dc+ [21].

The better efficiency of pulsed+ corona with respect to dc corona of either polarity is consistent with the results of an emission spectroscopy study which showed that at any specific input energy significantly greater average electron energy is obtained with pulsed corona than with dc coronas [25]. Correspondingly, a higher density of reactive O atoms is observed in pulsed + corona than with dc coronas [25]. Due to the filamentary nature of the plasma, not only the energy but also the spatial distribution of electrons and other short-lived reactive species is very different from that in glow dc coronas: the plasma is affecting a relatively larger volume thus accounting for a more efficient process.

A second important variable is the VOC initial concentration. Usually, the corona induced oxidation efficiency decreases as the VOC initial concentration $[X]_0$ is increased and often a

http://dx.doi.org/10.5772/60049

linear correlation is observed between k_E and $1/[X]_0$ within a significant range of concentrations. An example is shown in Figure 5.

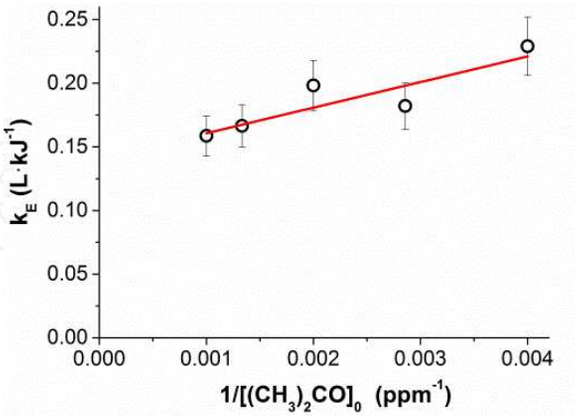

Figure 5. Dependence of process efficiency (k_E) on the reciprocal of VOC initial concentration for dc+ corona induced oxidation of acetone in dry synthetic air.

Other similar cases are reported in the literature [14, 24, 26–29] and have been interpreted based on a simple scheme of inhibition by the intermediates formed in the VOC reaction [30]. Finally, the VOC chemical composition and structure also matters and different VOCs are oxidized with different efficiencies under the same experimental conditions. A few representative data are reported in Table 1.

VOC[b)]	dc–		dc+	
	dry air	humid air	dry air	humid air
n-hexane [c)]	$7.7 \cdot 10^{-1}$	1.1	$2.0 \cdot 10^{-1}$	$1.8 \cdot 10^{-1}$
i-octane	$4.2 \cdot 10^{-1}$	$7.5 \cdot 10^{-1}$	$1.3 \cdot 10^{-1}$	$1.2 \cdot 10^{-1}$
toluene	$4.1 \cdot 10^{-1}$	$8.1 \cdot 10^{-1}$	$1.4 \cdot 10^{-1}$	$1.3 \cdot 10^{-1}$
CH_2Br_2	$2.1 \cdot 10^{-1}$	$2.6 \cdot 10^{-1}$	$6.4 \cdot 10^{-2}$	$5.1 \cdot 10^{-2}$
CF_2Br_2	$1.4 \cdot 10^{-1}$	$1.1 \cdot 10^{-1}$	$4.5 \cdot 10^{-2}$	$3.9 \cdot 10^{-2}$

[a)] Data are from ref. [27] unless otherwise specified. [b)] VOC initial concentration was 500 ppm. [c)] Data from ref. [25].

Table 1. Reaction efficiency data, expressed as k_E in L kJ^{-1} units, for corona processing of different VOCs in dry and in humid (40% RH) synthetic air.

This outcome might not have been anticipated *a priori* since the generally accepted notion is that plasma chemical processes proceed via radical reactions which are usually very fast and poorly selective. This is the case, for example, for the reaction of OH radicals with organic compounds which is viewed as a major contributor to VOC oxidation in humid air plasmas.

The data in Table 1 show instead that air plasmas are somewhat selective. This selectivity might originate from either of two circumstances (or possibly a combination of the two): within a given type of plasma, say that produced by dc–, different VOCs either react along different

paths or react with the same species but at different rates. The vast available bibliography on rate constants for reactions of many VOCs with air plasma reactive species (atoms, radicals, ions) and on ionization energies and electron affinities provides tools to exclude some possibilities and sort out which reactions are most likely paths. Chemical knowledge and intuition help in providing model VOCs to be used as reactivity probes.

A most intriguing and informative response is found in studying the effect of humidity on the efficiency of VOCs oxidation. The data in Table 1 show that for all VOCs considered, except CF_2Br_2, the presence of humidity in the air produces an increase in efficiency with dc– corona and no effect or a slight decrease in efficiency with dc+ corona. The increase in efficiency observed with dc– is rather straightforwardly attributed to the OH radicals formed by corona discharges in humid air. OH radicals are among the strongest known oxidants of VOCs. Compare for example the rate constants for reaction of toluene with atomic oxygen (2) [31] and with OH radical (3) [32], a channel becoming more available in humid air plasma:

$$C_7H_8 + O \rightarrow Products \qquad k_{298} = 7.6 \cdot 10^{-14}\ cm^3 \cdot molecule^{-1} \cdot s^{-1} \tag{2}$$

$$C_7H_8 + OH \rightarrow Products \qquad k_{298} = 5.7 \cdot 10^{-12}\ cm^3 \cdot molecule^{-1} \cdot s^{-1} \tag{3}$$

Support for the conclusion that reaction with OH radicals is important in dc– corona induced oxidation of hydrocarbons and of CH_2Br_2 (Table 1) came from experiments with CF_2Br_2 (halon 1020) [27]. Like other perhalogenated saturated hydrocarbon, CF_2Br_2 is not attacked by OH and other atmospheric radicals: the reaction of CF_2Br_2 with OH radicals is more than 220 times slower [33] than that of CH_2Br_2. And indeed there was no increase in efficiency for dc– processing of CF_2Br_2 in humid air, but rather a slight decrease with respect to dry air. This slight decrease in efficiency was attributed to reaction (4) which contributes to reduce the average electron energy while producing OH radical, which is unable to attack this specific VOC.

$$H_2O + e^- \rightarrow OH + H + e^- \tag{4}$$

Less straightforward was to explain the decrease in efficiency observed with dc+. To make sure that OH radicals also form in dc+ corona regime and to compare their relative densities in dc + and dc– air plasmas the well known reaction of OH with CO to form CO_2 (eq. (5)) was used [34].

$$CO + OH \rightarrow CO_2 + H \qquad k_{298} = 2.41 \cdot 10^{-13}\ cm^3 \cdot molecule^{-1} \cdot s^{-1} \tag{5}$$

Indeed, in a control experiment CO did not react at all in dry air under the effect of either dc + or dc– corona. In contrast, in humid air (40% RH) reaction (5) occurs both with dc–, more efficiently, but also with dc+ corona, thus proving the presence of OH radicals in such plasmas. Since with dc+ oxidation of hydrocarbons is less efficient in the presence of OH radicals than it is in dry air (Table 1), it was concluded that reaction with OH radicals is not the dominant initiation channel for their oxidation in dc+ corona. Thus, it appears clearly that VOC oxidation

induced by dc+ and dc– corona in air occurs by different mechanisms. For the investigated hydrocarbons (see Table 1) oxidation induced by dc+ corona is believed to be initiated by ion-molecule reactions. Support for this hypothesis comes from direct observation of the ions within the plasma achieved by APCI-mass spectrometry analysis and from comparison of current/voltage (I/V) profiles measured with only synthetic air and with VOC-containing synthetic air.

Figure 6 (a) reports *I/V* data monitored in experiments with toluene (500 ppm initial concentration). It is seen that for dc– the profiles determined with and without toluene are nearly superimposed, whereas in the presence of toluene for dc+ the current intensity measured is significantly lower, at any applied voltage, than found in pure synthetic air. Since corona current is due to ion transport across the drift region of the interelectrode gap, the results suggest that with dc+ corona different ions are present in pure air and in toluene containing air. Accordingly, different average ion mobilities are derived from the current/voltage characteristics of Figure 6 (a) [35–37]: 2.35 $cm^2 \cdot V^{-1} \cdot s^{-1}$ for pure air and 1.79 $cm^2 \cdot V^{-1} \cdot s^{-1}$ for toluene-containing air, respectively.

APCI-mass spectrometry is a powerful tool for monitoring and characterizing the ions formed by corona discharges and their reactions. The APCI-mass spectra reported in Figure 6 (b) show the ions present in the plasma produced in synthetic air by dc– and dc+ corona discharge, respectively. These ions are water clustered O_2^- and O_3^- ions ($O_2^-(H_2O)_n$ (n = 0-2: m/z 32, 50, 68), $O_3^-(H_2O)_n$ (n = 0-1: m/z 48, 66)) as well as $O_2^-(O_2)$ (m/z 64) for dc– corona and $H_3O^+(H_2O)_n$ (n = 2 - 3: m/z 55, 73) and $NO^+(H_2O)_n$ (n = 1 - 2; m/z 48, 66) for dc+ corona, respectively.

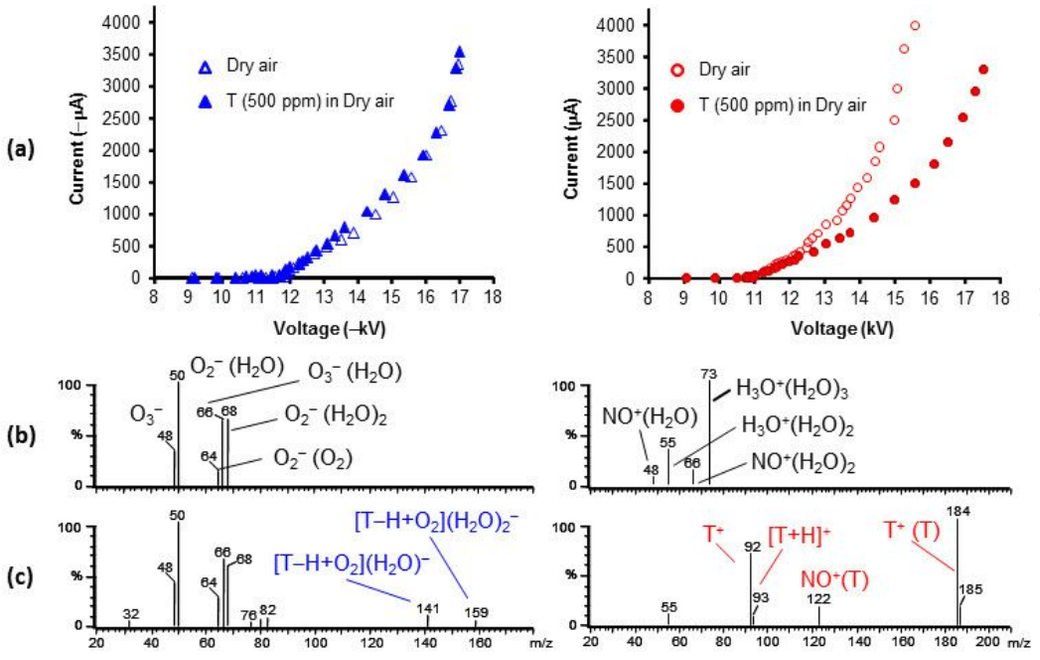

Figure 6. (a) Current/voltage profiles measured with dc– and with dc+ corona in pure air (open symbols) and in toluene (500 ppm) containing air (closed symbols). (b) APCI mass spectra recorded with dc– and dc+ corona in pure air. (c) APCI mass spectra recorded with dc– and dc+ corona in air containing toluene (500 ppm).

The APCI mass spectra recorded under the same experimental conditions except for the presence of a small amount of toluene (500 ppm) in the air are shown in panel (c) of Figure 6. The effects are significantly different for dc– and dc+ corona. Thus, with dc– corona the major ions observed in the plasma are the same regardless of whether toluene is present or not in the gas (compare the mass spectra on the left-hand side in panels (b) and (c) of Figure 6). These observations are fully consistent with and provide a rationale for the nearly identical *I/V* curves determined for dc– in pure air and in toluene containing air (panel (a) of Figure 6).

In contrast, in the case of dc+ the mass spectrum of toluene containing air is completely different from that of pure air (compare the mass spectra on the right-hand side in panels (b) and (c) of Figure 6). Thus, in air contaminated with toluene (500 ppm) the prevailing charged species are T^+ (m/z 92) and $[T+H]^+$ (m/z 93) (T stands for the toluene molecule), along with their ion-molecule complexes $T^+(T)$ (m/z 184) and $[T+H]^+(T)$ (m/z 185). These ions form [38-40] via exothermic charge- and proton transfer ion-molecule reactions (eq. 6 and 7), characterized by rate constants of 1.8×10^{-9} and 2.2×10^{-9} cm^3 $molecule^{-1}$ s^{-1}, respectively [38], followed by ion-molecule complex formation (eq. 6a and 7a).

$$\begin{aligned} T + O_2^+ &\rightarrow T^+ + O_2 \\ T^+ + T + M &\rightarrow T^+(T) + M \quad (a) \end{aligned} \tag{6}$$

$$\begin{aligned} T + H_3O^+ &\rightarrow [T+H]^+ + H_2O \\ [T+H]^+ + T + M &\rightarrow [T+H]^+(T) + M \quad (a) \end{aligned} \tag{7}$$

Finally, the $NO^+(T)$ (m/z 122) ion-molecule complex is also observed. Thus, mass spectroscopic ion analysis provides a rationale, at the molecular level, for interpreting *I/V* curves observed with dc+ (Figure 6 panel (a) right hand side). In addition, these results suggest that ionic reactions might be responsible for the initial stages of toluene decomposition induced by dc+ corona. This hypothesis is consistent with the observed insensitivity of the dc+ process efficiency to the presence of humidity, which rules out a significant role of the OH radical.

Analogous results were obtained with other hydrocarbons leading to the conclusion that the initial step of oxidation depends on the plasma regime applied: ion-molecule reactions are favored with dc+ whereas reactions with O atoms and OH radicals prevail in the case of dc– corona discharges.

The yield of the final oxidation product, CO_2, as a function of SIE has been determined and compared with the profile of VOC conversion (Figure 7). CO_2 production is clearly less energy efficient than VOC conversion as is reasonable to expect for a process which involves many steps and oxidation intermediates.

In comparing pulsed and dc coronas, at any given value of VOC conversion the yield of CO_2 increases in the order pulsed+ < dc– < dc+. This is evident from the data shown in Figure 8a concerning experiments with *n*-hexane. Comparing the results corresponding to a given

http://dx.doi.org/10.5772/60049

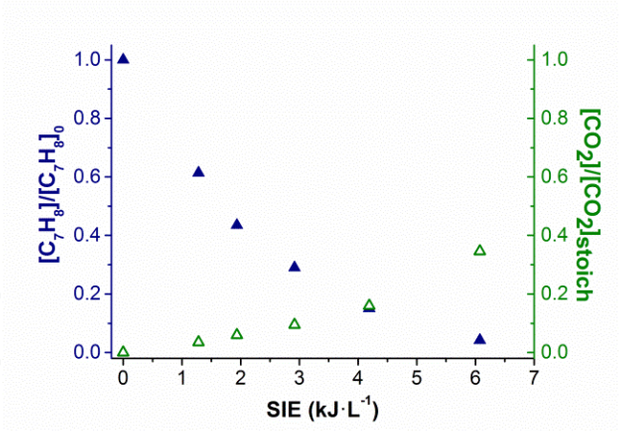

Figure 7. Profiles of VOC decay and CO_2 production as a function of SIE for treatment of toluene (500 ppm) with dc– corona in dry synthetic air.

decomposition fraction of the VOC, for example 0.7 (70% conversion), the corresponding amount of CO_2 released with dc+ is about 4 times larger than with pulsed+ and about 1.6 times larger than with dc–. Thus, among the different types of corona tested, dc+ has the poorest efficiency for VOC conversion but the best selectivity for CO_2 production. On the other hand, a consistently lower CO_2/CO ratio is found with dc+ than with dc– and pulsed+ (Figure 8b).

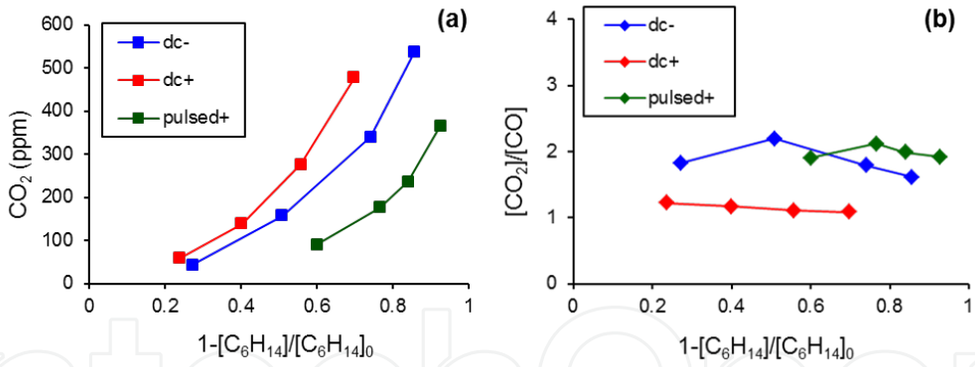

Figure 8. CO_2 production and CO_2/CO ratio for treatment of *n*-hexane (500 ppm) with dc+, dc– and pulsed+ corona in dry synthetic air. The data are displayed as a function of the fraction of decomposed *n*-hexane.

In search for the missing fraction of organic carbon several oxidation intermediates were identified and quantified by means of GC/MS and GC/FID analysis and proper standards. In the case of *n*-hexane the major detected intermediates were a few aldehydes and ketones, as shown in Figure 9. It is seen that the concentration of most of these intermediates reaches a maximum and then decays, showing that they are in turn oxidized in air non-thermal plasmas. It is also seen that, with the exception of acetaldehyde, the concentrations of these organic intermediates are very small under any of the applied conditions. The experimental data have been fitted according to a simple kinetic model for consecutive reactions [41] to obtain relative reactivity data of the intermediates with respect to that of the precursor, *n*-hexane [18].

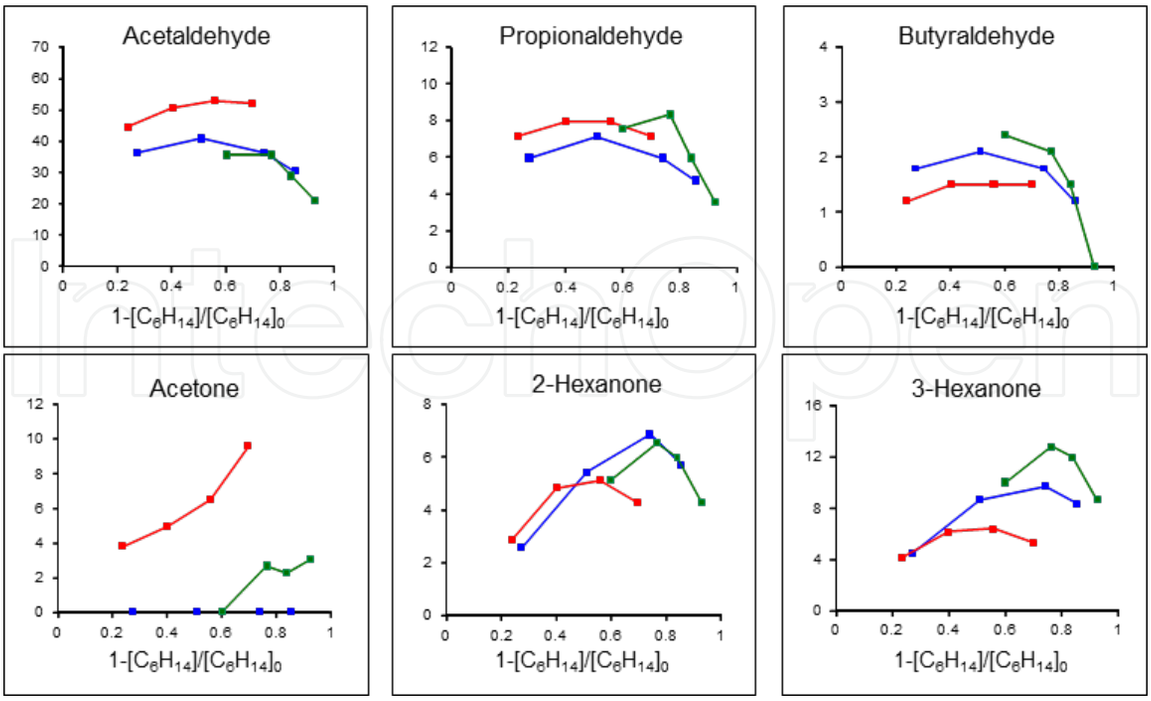

Figure 9. Aldehydes and ketones detected as intermediates in the oxidation of *n*-hexane (500 ppm in dry synthetic air) induced by pulsed+, dc– and dc+. The data are displayed as a function of the fraction of decomposed *n*-hexane [18].

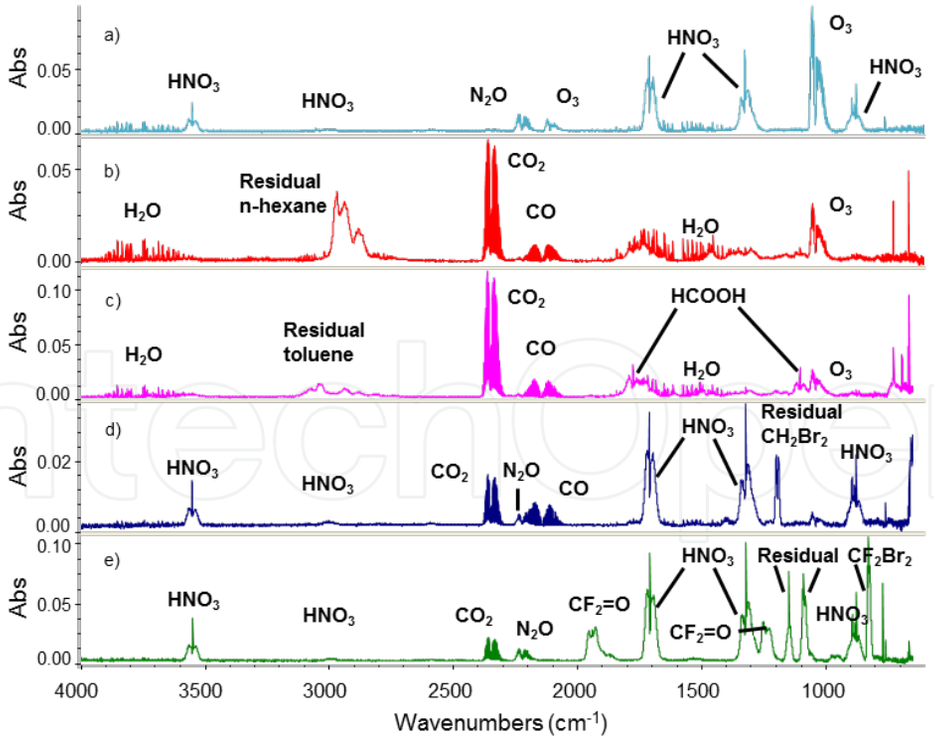

Figure 10. FT-IR spectra recorded in experiments with dc+ corona (+19 kV) in (a) pure synthetic air, used as reference spectrum, and in synthetic air containing 500 ppm of the following VOCs: (b) *n*-hexane; (c) toluene; (d) CH_2Br_2; (e) CF_2Br_2.

In line FT-IR spectroscopy gives a comprehensive overview of the composition of the treated gas analyzed at the outlet of the corona reactor. Besides CO_2 and CO, other species can be conveniently determined, including ozone, various nitrogen oxides and derivatives (N_2O, HNO_3, etc), and, depending on the specific VOC, also other volatile organic oxidation intermediates. A few examples, reported in Figure 10, show characteristic bands for VOC specific products such as formic acid in the case of toluene and CF_2O in the case of CF_2Br_2.

The production of HNO_3 is high and ozone is almost completely absent in corona discharge treatment of air containing bromo derivatives CH_2Br_2 and CF_2Br_2, (Figure 10 d and e). These observations have been explained considering reactions and catalytic cycles involving BrOx (x = 0, 1) and NOx (x = 1, 2) species [24], which have been extensively investigated as major contributors to the depletion of stratospheric ozone [42].

4. VOC removal by means of barrier discharges

The experimental results obtained with a surface DBD reactor developed at INP Greifswald are reported. The discharge arrangement consists of two metal woven meshes and a dielectric plate (mica) in between the two electrodes [43]. As shown in Figure 11 the surface DBD arrangement (110 x 80 x 3 mm) was installed in a gastight chamber made of poly(methyl methacrylate) (PMMA) where the gas mixture to be treated (mixed from gas cylinders by means of mass flow controllers) was conveyed with a total gas flow of 75 L_N/h. In order to vary the humidity of the gas mixture the partial gas flow from oxygen gas cylinder was directed through a water containing bubbler. Water content of around 0.5% was realized in this way. Most of the gas flows along the electrodes configuration instead of entering the active plasma region between the electrodes and the dielectric as depicted by the arrows in Figure 11 (right). An advantage of this configuration is the very small back pressure, which is desired for the treatment of large gas flows.

The plasma reactor was energized with a programmable high-voltage power source and a high-voltage transformer. The frequency of the applied voltage was ranged from 400 Hz to 1 kHz. The power dissipated into the plasma was analyzed by recording the high voltage operating the reactor via a high voltage probe. Additionally, the voltage drop over a capacitor (capacitance 100 nF), connected in series with the reactor between the grounded electrode and protected earth, was recorded. By multiplying the voltage drop over the capacitor by the capacitance the transferred charge was obtained.

Samples of the gas mixture were analyzed by Flame Ionization Detector (FID) (Testa FID-2010T), measuring the total amount of organic carbon present in the exhaust gas. Additionally, a Fourier Transform InfraRed spectrometer (FTIR) (Bruker Alpha, spectral resolution 1 cm^{-1}, optical path length 5 m) was used to monitor the processed gas mixtures. The gas cell of the spectrometer was heated up to 40°C in order to avoid water condensation. Higher temperatures would be desirable to avoid water condensation but cannot be used otherwise ozone will decompose and give rise to sort of a "post-plasma" contribution to toluene oxidation which should be avoided.

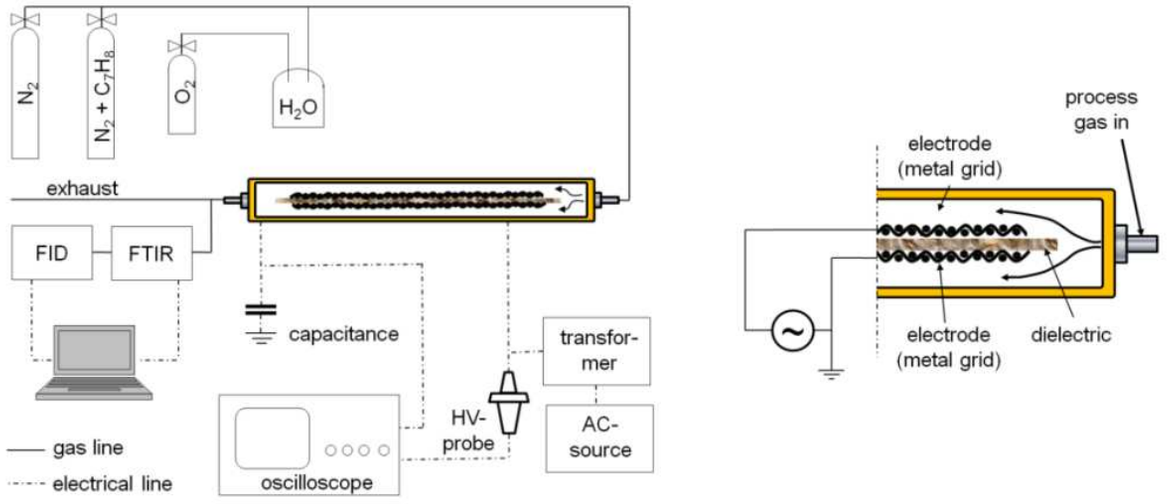

Figure 11. Experimental setup for toluene removal studies (left) and detailed horizontal cut view of the Surface DBD reactor (right).

In order to obtain comparable results of the measurements under the selected conditions the operating voltage was chosen as the electrical parameter to be set for every measurement. The electrical data recorded during the experiments were investigated during the analysis procedure. The power input into the plasma reactor was calculated by integrating the area of the charge-voltage plot (Q-V plot) and multiplying the resulting value with the frequency of the applied voltage [44]. By this, it was found that the Q-V plots for different frequencies at the same driving voltage were almost identical.

Examples are given in the left part of Figure 12. The black curves show the Q-V plots recorded at a frequency of 400 Hz, whereas the red curves display that one recorded at 1 kHz. The operating voltage was 8.3 kV and 6.9 kV, respectively. The equality of the Q-V plots implies that the energy transferred per cycle into the plasma is almost identical. Thus, the power input for a fixed operating voltage should depend only on the frequency in a linear relation [44]. Using the frequency ratio 2.5 (1000 Hz divided by 400 Hz) and multiplying it with the power input measured at 400 Hz, one gets the calculated power at 1 kHz. In the right part of Figure 12 the power measured at 400 Hz (black boxes), the power calculated for 1 kHz (blue triangles) and the power measured at 1 kHz (red circles) are shown. The values calculated and measured at 1 kHz are in good agreement and can be taken as another evidence of the proportionality of frequency and power, as already mentioned by Kogelschatz [44] and Manley [45].

Further investigations showed that the slope from the bottom right corner to the upper right one of the charge-voltage plot, which gives the capacitance of the plasma reactor during the discharge period, increases with increasing the operating voltage (Figure 13, left). The reason is suggested to be the increase in the active area of the electrode, which means the surface of the electrode covered with plasma. Photographs of the plasma were taken (Nikon D5100, aperture 5.6, exposure time 30 s) and reworked with an image manipulation program (Gimp 2.8, color correction) to make the plasma visible (Figure 13, right). An analysis of the extension of the visible plasma was performed. The obtained values were normalized as well as the

http://dx.doi.org/10.5772/60049

values of the measured capacitance. The result is given in the left part of Figure 13. The normalized capacitance (red circles) increases linearly with the increasing driving voltage. The normalized active area of the plasma (black boxes) increases almost linearly, except the value at 7.3 kV. The linear relation between the dielectric capacitance and the amplitude of the applied voltage is further confirmed by the fact that the bottom right corner as well as the left top corner of the Q-V-plot (which both correspond to the inset of the discharge in every half period of the applied voltage) are not sharp. This would be the case for a uniform breakdown of the gas discharge.

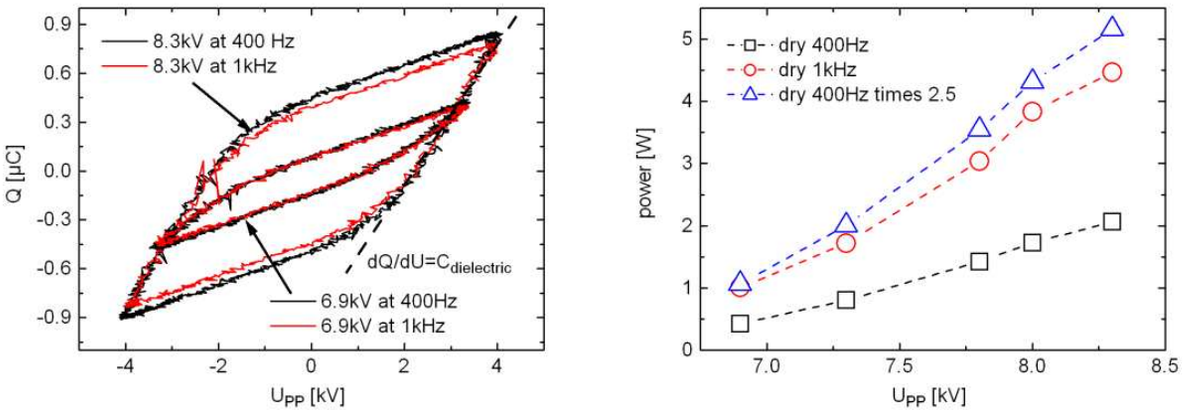

Figure 12. Left: Q-V plots recorded at 8.3 kV and 6.9 kV at 400 Hz and 1 kHz under dry conditions. Right: Power input under dry conditions at 400Hz and 1 kHz and at 1 kHz calculated based on the power of 400 Hz.

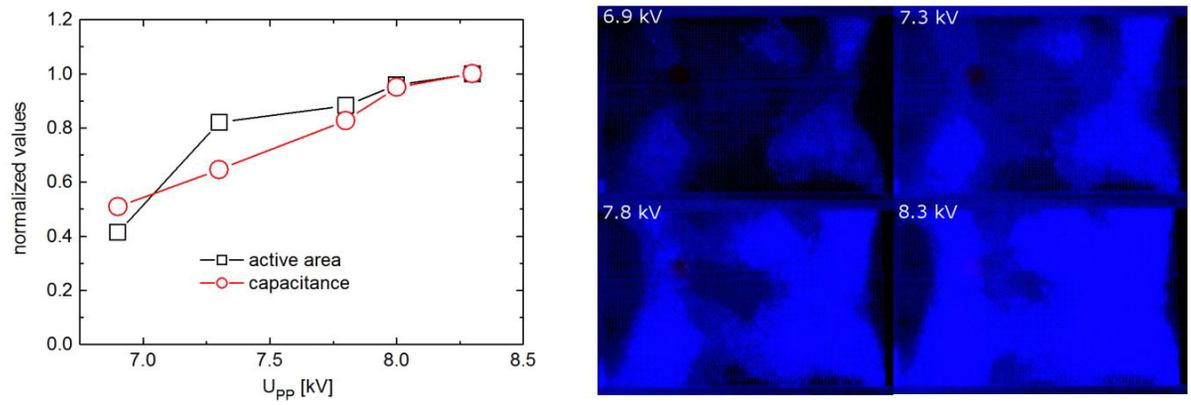

Figure 13. Left: Increase in active plasma area and increase in capacitance with respect to the operating voltage. Right: Photographs of the plasma operated at different voltages.

In a first step the overall plasma chemistry of toluene removal was investigated by FTIR. In Figure 14 samples of selected spectra are presented showing the so-called fingerprint region (i.e. wavenumber 700–1500 cm^{-1}). The left graph shows infrared-spectra taken at an applied voltage amplitude of 8.3 kV_{PP} and a frequency of 400 Hz under dry conditions. In the untreated gas mixture (black curve) the absorption band related to toluene is the only detectable band.

With plasma (red curve) the strong absorption band of ozone appears at 1053 cm^{-1}, which is the main stable by-product of an NTP operated under ambient air conditions. Additionally, nitric acid HNO_3 is detected. It is assumed that HNO_3 is formed by the reaction of intermediate NO_x with hydroxyl radicals produced by the toluene decomposition. The toluene absorption band is replaced by a broad absorption band whose origin could not be identified. Because no infrared absorption spectrum of the known products or intermediates (formaldehyde, benzaldehyde, benzoic acid, benzene, nitrobenzene, phenol, formic acid, and acetic acid) of the toluene removal process fits to the measured spectra it is assumed that it is a compound emitted from the material of the reactor housing (PMMA). According to the results given by the FID this analyzed gas mixture does not contain any hydrocarbons at all.

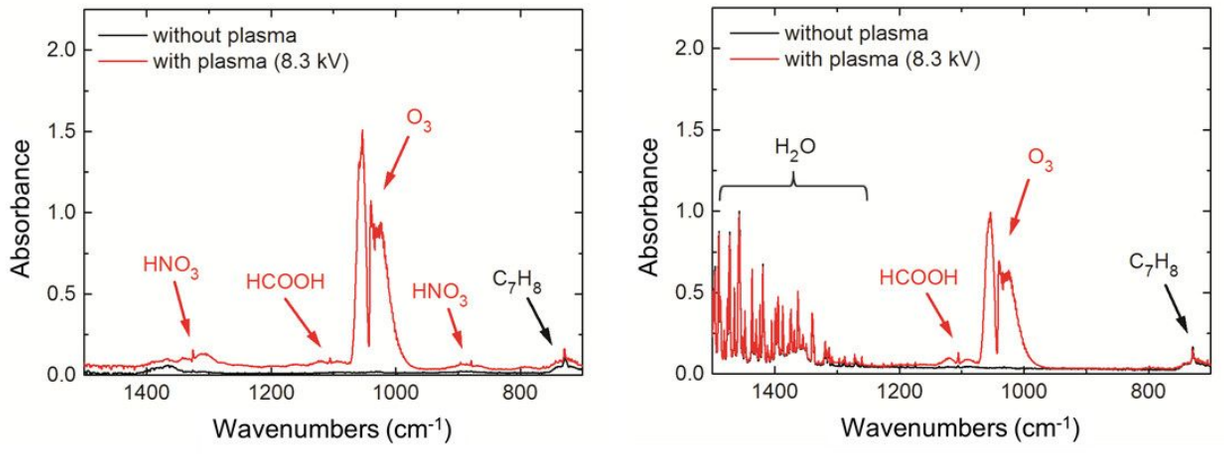

Figure 14. FTIR absorption spectra without plasma (black lines) and with plasma (frequency 400 Hz, operating voltage 8.3 kV, red lines) under dry (left) and wet conditions (right) of 50 ppm toluene in synthetic air.

Under wet conditions (right graph, same electrical parameters) there is no nitric acid detectable. Moreover, the absorption of ozone is much smaller than under dry conditions. Both phenomena are attributed to the consumption of energetic electrons, which under dry conditions are used to produce NOx as a necessary intermediate for the production of nitric acid. These changes result in a considerable production of formic acid. The lower energy efficiency in toluene removal under wet conditions is also assumed to be due to the consumption of high energy electrons for the vibrational excitation of water.

FID is used to study the toluene removal since it is not sensitive to the main by-products of toluene removal that were identified by FTIR. With the concentration of toluene at about 50 ppm in the untreated gas mixture the molar fraction was calculated and plotted against the SIE. The results are shown in Figure 15. The removal efficiency increases with the SIE up to total removal at around 55 $J \cdot L^{-1}$ under dry conditions (black boxes). The same efficiency is achieved for 400 Hz and 1 kHz. Under wet conditions (red circles) the removal efficiency is smaller and about twice as much energy is needed to achieve complete removal of toluene which is only obtained at 1 kHz for this conditions. This dependency on the frequency is only found under wet conditions.

http://dx.doi.org/10.5772/60049

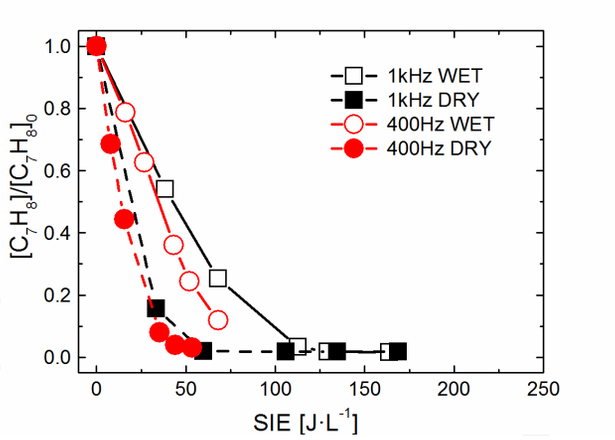

Figure 15. Molar fraction of toluene under dry (black boxes) and wet (red circles) conditions at 400 Hz (circle) and 1 kHz (square).

In order to discuss the energy efficiency the energy constant parameter k_E was evaluated according to the eq. (1). As reported in Table 2 the energy constants obtained under dry conditions are very similar. Those obtained under wet conditions are significantly smaller but also differ significantly.

Frequency	k_E L·J^{-1}	
	dry	wet
400 Hz	$5.85 \cdot 10^{-2}$	$3.03 \cdot 10^{-2}$
1 kHz	$5.63 \cdot 10^{-2}$	$2.06 \cdot 10^{-2}$

Table 2. Reaction energy efficiency data, expressed as k_E in L J^{-1} units, for DBD processing of toluene.

Quantitative analysis data for CO_2 and CO produced under different experimental conditions are shown in Figure 16 as a function of the SIE. At dry conditions the production of CO is favored compared to CO_2, while in humid conditions the amounts of both compounds are almost the same. The increased selectivity towards CO_2 in humid conditions could be explained as follows. In the presence of water vapor in the plasma area the production of OH radicals is higher. These radicals can react with the CO molecules to produce CO_2, according to the eq. (5).

Usually the formation of OH radicals in the plasma area is also accompanied by an enhancement of the energy efficiency in the VOC removal process (e.g. see **Section 3** of this Chapter). In the case of this setup, as discussed above, the presence of water vapor in the process gas is obviously responsible of a decrease in the energy efficiency of toluene removal.

In Figure 17 the selectivity to CO_2 of the plasma treatment for pollutant degradation is reported. The black vertical line is referred to a value of SIE of 55 J·L^{-1}, the energy value at which the toluene is completely decomposed, but as reported in Figure 17 there is selectivity of 40% in dry conditions and of 60% in humid conditions. The complete oxidation of the toluene is

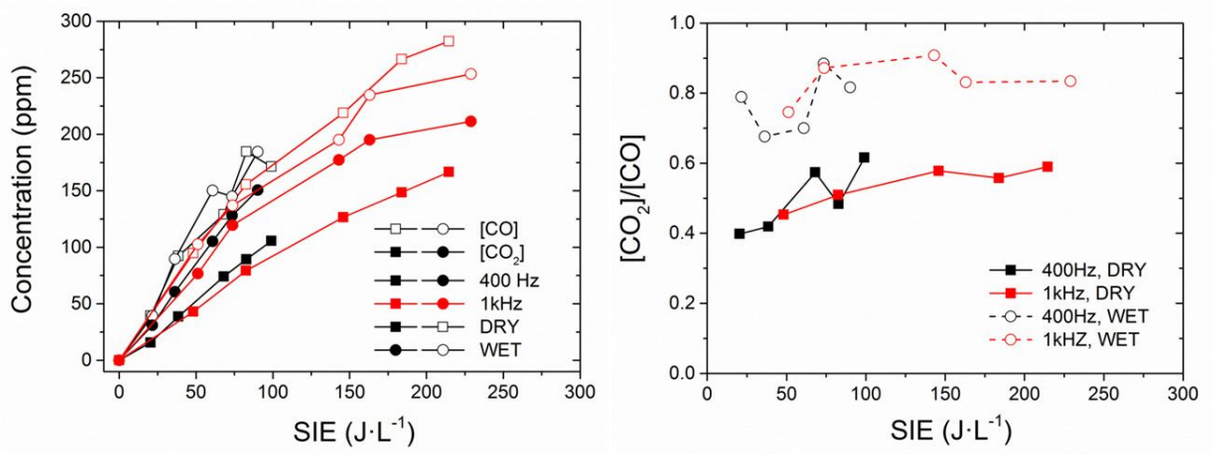

Figure 16. Left: CO (empty symbols) and CO_2 (full symbols) production during toluene decomposition experiments. Comparison at 400 Hz (black) and 1 kHz (red) and between dry conditions (full line) and wet conditions (dashed line). Right: CO_2/CO ratio as a function of SIE at 400 Hz (black) and 1 kHz (red). Comparison between dry condition (full symbols and straight lines) and humid conditions (empty circle symbols).

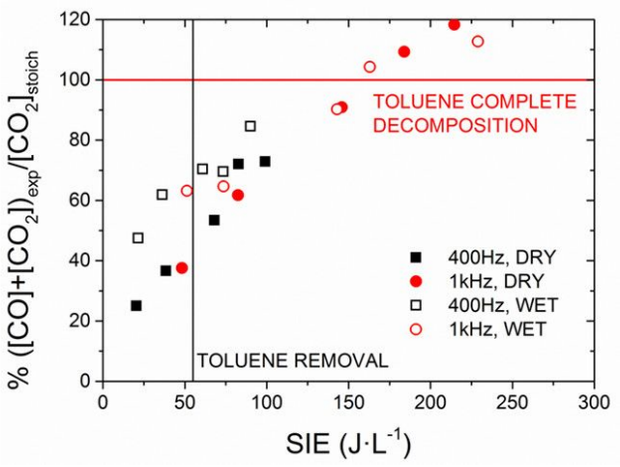

Figure 17. Carbon balance for the different experimental conditions being tested. 400 Hz (black symbols) and 1 kHz (red symbols) under dry (full square symbols) and wet (empty symbols and dashed lines) conditions.

achieved at a value of SIE of 150 J·L^{-1}, where all the VOC is decomposed to CO and CO_2. The carbon fraction which is missing is mainly formic acid that could be easily removed from the effluent gas by means of water scrubbing. Despite the reduction of the toluene removal efficiency made by the presence of water vapor, it is clear how the selectivity to CO_2 production is improved (Figure 16, right), but also the carbon balance is clearly improved at least until the energy value of 100 J·L^{-1}. Above the value of 150 J·L^{-1} the carbon balance is exceeding 100% (marked by the red horizontal line). This is due to some additional degradation of the acrylic housing. This effect was also noted in the IR spectra where an additional band around 700 cm^{-1} was recorded (see Figure 14).

Because of the construction of the NTP-reactor with the electrode configuration in the middle of the discharge reactor and, therefore, a huge gas volume not in direct contact with plasma,

http://dx.doi.org/10.5772/60049

the toluene to be removed hardly comes in contact with plasma. Thus, electron dissociation cannot be the main process. As ozone is generated in the air plasma it is a possible oxidizer of toluene. The effect of ozone on the toluene removal has been studied in a separate experiment. Therefore the reactor was operated with a pure oxygen gas flow which was mixed with the toluene polluted air in a separate reaction chamber (volume about 250 mL; not shown in Figure 11). The results of this experiment are presented in Figure 18.

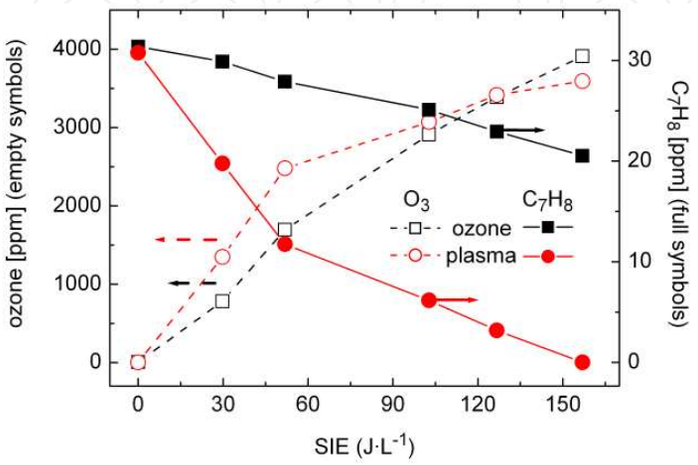

Figure 18. Ozone and toluene concentrations as a function of SIE (frequency 1 kHz) at the surface DBD arrangement. Comparison of the direct plasma treatment (red symbols) with the ozone injection experiment (black).

Ozone concentration increases and toluene concentration decreases with increasing SIE. The ozone production is similar in both direct discharge and ozonation treatments, but the toluene removal varies significantly. In the case of indirect treatment with ozone a small reduction of toluene is obtained. In additional experiments a similar reduction was obtained even without plasma operation. Thus it must be that toluene is adsorbed somewhere in the system (reaction chamber, pipes etc). In case of direct treatment at 157 JL^{-1} toluene is completely removed. These results show that reactions with ozone are not dominant, which is in agreement with the fact that the rate coefficient of the reaction of toluene with ozone is small (eq. (8) [46]) compared to the reaction with atomic oxygen (eq. (2)).

$$C_7H_8 + O_3 \rightarrow Products \qquad k_{298} = 1.5 \cdot 10^{-22}\ cm^6 \cdot molecule^{-1} \cdot s^{-1} \tag{8}$$

The reaction with atomic oxygen (eq. (2)) is considered to be the most important removal process.

Since for the production of these species energetic electrons are needed, the lower efficiency under wet conditions can be explained by their lower production efficiency due to the consumption of these electrons as well as a reduction of the electron temperature by water dissociation and vibrational excitation. More detailed investigation on the toluene by-products are needed to clarify the carbon balance and the selectivity of the process which remains to future investigations.

5. Conclusions and outlook

The feasibility of NTP for the removal of VOCs has been demonstrated by means of two different gas discharge concepts, namely DBD and corona discharge. There are evident peculiarities in the two different approaches and, notably, also among different types of coronas. Different discharge regimes create NTPs with distinct properties and compositions (type and density of reactive species), which reflect on the process chemical outcome. This knowledge is important for mastering the process product selectivity, i.e. the chemical composition of the treated gas. Likewise important is the process efficiency. Unfortunately, up to now it is possible to make a comparison between the two reactor arrangements only for the specific case of toluene. There are reviews in the literature in which the efficiency of different NTP processes is compared [17].

Regarding the main chemical reaction involved in the decomposition process of toluene a similar mechanism for DBD and dc– corona can be proposed. Here, the most important reactive species are radicals. The main difference in the overall efficiency of the decomposition process is when water vapour is present in the treated gas, but this opposite effect is totally in agreement with the physical properties of the DBD. In the case of the DBD configuration the volume of gas which is directly affected by plasma is small compared to dc– corona. Accordingly, in the case of the corona a much higher probability of collisions between reactive species and substrate molecules (toluene) exists, but also a high probability to generate OH radicals. In the case of DBD the presence of water vapour is quenching the high energetic electrons and reducing the chance to generate more reactive species with an overall result of a decrease in energy efficiency. Despite this, if we calculate the Energy Yield (EY) according to the equation reported in [47]:

$$EY = \frac{C_{in} \cdot \eta \cdot M \cdot 0.15}{SIE} \tag{9}$$

where C_{in} is the starting concentration of the pollutant to be treated (ppm), η is the removal efficiency and M is the molar mass of the pollutants. For the DBD configuration EY value is 13.6 g/kWh while for the corona reactor, in pulsed+ mode, the value is 6.9 g/kWh.

Plasma type	Concentration range (ppm)	Maximum removal efficiency (%)	Energy Yield (g/kWh)
DBD (this work, sec. 4)	**50**	**>99**	**13.6**
DBD packed with glass pellets [47]	1100	80	11.5
Pulsed Corona (this work, sec. 3)	**500**	**>99**	**6.9**
DBD packed with glass beads [47]	240	36	6.8
DBD [47]	400	23	5.2
DC corona [47]	5 – 200	93	0.4

Table 3. Selected results on toluene removal with NTP in dry air.

http://dx.doi.org/10.5772/60049

In Table 3 are summarized selected results on toluene removal with NTP taken from [47] to better evaluate the EY of the two setups reported above. In general, the DBD setups present higher values compared to the corona ones. What is really interesting to note from this table is that not only the values of EY obtained with the setups developed by the authors are among the highest ones, but also these are the only cases in which the complete removal of toluene is reached.

In contrast to many other established technologies of air cleaning, NTPs can be controlled more or less instantaneously by their electrical operation parameters, and they can thus be adjusted to fluctuating gas flow volumes and/or contamination levels. However, nearly all practical processes of pollutant degradation in gases by means of NTPs are hybrid processes or a combination of NTPs with other technologies. In such combinations the NTP acts as an oxidation stage. However, the combination is not only a processing by means of subsequent methods but also offer multiple process synergies. Therefore NTP can be coupled with catalysts, adsorbing agents or scrubbing. For example, the oxidation of non-soluble VOCs results in soluble by-products such as formaldehyde or formic acid. This can also be used for the removal of NO_x [48]. The so-called Plasma Enhanced Selective Catalytic Reduction (PE-SCR) of NOx offers many synergies between plasma and catalyst.

In this context, the combination of plasma treatment with adsorption methods has also been proposed for VOC abatement and deodorization [49]. Several manufacturers offer devices for deodorization which sometimes combine a NTP with an active carbon or molecular sieve stage. The odour reduction of so-called indirect plasma treatment was also demonstrated. Indirect treatment means that the plasma processed air is injected in the VOC containing off-gas. In such case short lived radicals and ions may be less involved in the decomposition processes but the operation lifetime of such system is much longer. During the direct plasma decomposition aerosols can be formed by nucleation of intermediate products and deposit as layers on the electrodes which interfere with the plasma generation. This is avoided by indirect treatment. Many of such DBD-based installations are worldwide used for deodorization in several factories for producing food for fattening, fish meal and flavouring substances. The installations are low-maintenance and need about one third to one fifth of the space as conventional technologies. In [50] the investment- and running cost of numerous waste air purification processes for a gas flow of 50,000 m_N^3/h and for <100 mg VOC/m^3 in the flavour processing industry were determined and compared. NTP installation had the lowest investment costs (about 400,000 € compared to at least 700,000 € for combustive methods, biological filter or molecular sieve filtration) and second lowest operating cost (about 8 €/h, compared to 70 €/h for combustion and biological filtration with 35 €/h). Although the applicability of NTPs is devoted to low-contaminated gas streams, these examples show the high economic relevance and potential of such technologies.

Furthermore, the combination of NTP with absorbers offers the possibility to establish cyclic processes for the removal of low-concentrated pollutants [49]. In such processes, the low-concentrated pollutants are adsorbed and thus concentrated on solid matter in a storage phase. In the subsequent plasma phase, the adsorbed molecules are desorbed and decomposed by plasma activity. Since the retention time of the pollutants in the plasma phase and their concentration are increased, less energy is consumed in such a plasma-enhanced adsorption process. Such processes have been established to decompose different VOCs and NO_x, as

summarized in [51]. The decomposition of adsorbed ethanol on active carbon samples by means of ozone generated in the plasma has been investigated in [52]. The regeneration of clinoptilolite (a natural zeolite) loaded with NH_3 has recently been shown by means of a packed-bed DBD reactor. The adsorbed NH_3 is released at a relatively low temperature and low energy consumption [53]. A cycled adsorption and plasma process using mineral granulates consisting of 80 % halloysite in a packed-bed DBD reactor for the removal of formaldehyde CH_2O was investigated in [51]. Here, the adsorbed CH_2O molecules were decomposed into CO_X and hydrocarbons in N_2 plasma. The total amount of decomposed CH_2O and the selectivity towards CO_2 increased with N_2 gas space-times (i.e. the time required to process one packed bed volume of adsorbing material with gas) and with oxygen fraction in the carrier gas. The above examples demonstrate the high potential of plasma-enhanced techniques, which can increase efficiency and lower operational costs. However, more research and development are necessary in order to establish a wider industrial breakthrough.

Acknowledgements

The authors would like to thank Dr. Tomáš Hoder, Mr. Wolfgang Reich and Mr. Alexander Schwock for their support on this work.

The work is partly supported by the European Regional Development Fund, Baltic Sea Region programme 2007-2013 (project No 033, "Dissemination and Fostering of Plasma Based Technological Innovation for Environment Protection in The Baltic Sea Region", PlasTEP). The research leading to these results has received further funding from the European Union Seventh Framework Programme (FP7/2007-2013) under grant agreement n°316216.

Author details

Milko Schiorlin[1*], Cristina Paradisi[2*], Ronny Brandenburg[1], Michael Schmidt[1], Ester Marotta[2], Agata Giardina[2] and Ralf Basner[1]

*Address all correspondence to: milko.schiorlin@inp-greifswald; cristina.paradisi@unipd.it

1 Leibniz Institute for Plasma Science and Technology (INP Greifswald), Greifswald, Germany

2 Department of Chemical Sciences, University of Padova, Padova, Italy

References

[1] von Sonntag C, von Gunten U. Chemistry of ozone in water and wastewater treatment: from basic principles to applications, ed. Iwa Publ., London, 2012

[2] Kim HH. Nonthermal plasma processing for air-pollution control: A historical review, current issues, and future prospects. Plasma Process. Polym. 2004;1(2), 91–110. DOI: 10.1002/ppap.200400028

[3] Mizuno A. Industrial applications of atmospheric non-thermal plasma in environmental remediation. Plasma Phys. Contr. Fusion 2007;49, A1-A15. DOI: 10.1088/0741-3335/49/5A/S01

[4] Hammer T, Bröer S. Plasma Enhanced Selective Catalytic Reduction of NOx for Diesel Cars. SAE Technical Paper 982428, 1998, DOI:10.4271/982428.

[5] Chmielewski AG, Tymiński B, Licki J, Iller E, Zimek Z, Radzio B. Pilot plant for flue gas treatment-continuous operation tests. Rad. Phys. Chem. 1995;46(4-6) 1067–1070. DOI:10.1016/0969-806X(95)00322-O.

[6] Kogelschatz U, Eliasson B, Egli W. Dielectric-Barrier Discharges. Principle and Applications. J. Phys IV France 1997;7(C4), C4-47–C4-66. DOI: 10.1051/jp4:1997405

[7] Moreau E, Sosa R, Artana G. Electric wind produced by surface plasma actuators: a new dielectric barrier discharge based on a three-electrode geometry. J. Phys. D-Appl. Phys. 2008;41(11) 115204. DOI: 10.1088/0022-3727/41/11/115204.

[8] Holzer F, Roland U, Kopinke FD. Combination of non-thermal plasma and heterogeneous catalysis for oxidation of volatile organic compounds: Part 1. Accessibility of the intra-particle volume. Appl. Catal. B-Environ. 2002;38(3) 163–181. DOI:10.1016/S0926-3373(02)00040-1.

[9] Kraus M, Eliasson B, Kogelschatz U, Wokaun A. CO_2 reforming of methane by the combination of dielectric-barrier discharges and catalysis. Phys. Chem. Chem. Phys. 2001;(3) 294–300. DOI: 10.1039/B007015G.

[10] Nijdam S, van Veldhuizen E, Bruggeman P, Ebert U. An Introduction to Nonequilibrium Plasmas at Atmospheric Pressure. In: Parvulescu VI, Magureanu M, Lukes P. (ed.) Plasma Chemistry and Catalysis in Gases and Liquids. Weinheim: Wiley-VCH GmbH & Co. KGaG; 2012. p.1–44.

[11] Hoeben WFLM, Beckers FJCM, Pemen AJM, van Heesch EJM, Kling WL. Oxidative degradation of toluene and limonene in air by pulsed corona technology. J. Phys. D: Appl. Phys. 2012;45, 055202. DOI: 10.1088/0022-3727/45/5/055202.

[12] Kozlov KV, Wagner HE, Brandenburg R, Michel P. Spatio-temporally resolved spectroscopic diagnostics of the barrier discharge in air at atmospheric pressure. J. Phys. D: Appl. Phys. 2001; 34(21), 3164–3176. DOI:10.1088/0022-3727/34/21/309.

[13] Hoder T, Černák M, Pailliol J, Loffhagen D, Brandenburg R. High-resolution measurements of the electric field at the streamer arrival to the cathode: A unification of the streamer-initiated gas-breakdown mechanism. Phys. Rev. E. 2012;86, 055401. DOI: 10.1103/PhysRevE.86.055401.

[14] Fridman A. Plasma Chemistry. Cambridge: Cambridge University Press; 2008.

[15] Urashima K, Chang JS. Removal of volatile organic compounds from air streams and industrial flue gases by non-thermal plasma technology. IEEE Trans. Dielec. Electric. Insul. 2000;7(5), 602–614. DOI: 10.1109/94.879356.

[16] Isbell MA, Stolzberg RJ, Duffy LK. Indoor climate in interior Alaska: simultaneous measurement of ventilation, benzene and toluene in residential indoor air of two homes. Science Total Environ. 2005;345(1-3), 31–40. DOI: 10.1016/j.scitotenv.2004.11.016.

[17] Vandenbroucke AM, Morent R, De Geyter N, Leys C. Decomposition of Toluene with Plasma-catalysis: A Review. J. Adv. Oxid. Technol. 2012;15(2), 232–241.

[18] Marotta E, Callea A, Rea M, Paradisi C. DC corona electric discharges for air pollution control. Part 1. Efficiency and products of hydrocarbon processing. Environ. Sci. Technol. 2007;41(16), 5862–5868. DOI: 10.1021/es0707411.

[19] Marotta E, Callea A, Ren XW, Rea M, Paradisi C. DC corona electric discharges for air pollution control, 2-ionic intermediates and mechanisms of hydrocarbon processing. Plasma Process. Polym. 2008;5(2), 146–154. DOI: 10.1002/ppap.200700128.

[20] Marotta E, Callea A, Ren XW, Rea M, Paradisi C. A Mechanistic Study of Pulsed Corona Processing of Hydrocarbons in Air at Ambient Temperature and Pressure. Int. J. Plasma Environ. Sci Technol. 2007;1(1), 39–45. http://www.iesj.org/html/service/ijpest/vol1_no1_2007/7_Marotta.pdf.

[21] Schiorlin M, Marotta E, Rea M, Paradisi C. Comparison of Toluene Removal in Air at Atmospheric Conditions by Different Corona Discharges. Environ. Sci. Technol. 2009;43(24), 9386–9392. DOI: 10.1021/es9021816.

[22] Marotta E, Scorrano G, Paradisi C. Ionic reactions of chlorinated volatile organic compounds in air plasma at atmospheric pressure. Plasma Process. Polym. 2005;2(3), 209–217. DOI: 10.1002/ppap.200400047.

[23] Donó A, Scorrano G, Paradisi C. Abatement of volatile organic compounds by corona discharge, a study of the reactivity of trichloroethylene under atmospheric pressure ionization conditions. Rapid Commun. Mass Spectrom. 1997;11(15), 1687–1694. DOI: 10.1002/(SICI)1097-0231(19971015)11:15<1687::AID-RCM33>3.0.CO;2-Y.

[24] Schiorlin M, Marotta E, Dal Molin M, Paradisi C. Oxidation Mechanisms of CF_2Br_2 and CH_2Br_2 Induced by Air Nonthermal Plasma. Environ. Sci. Technol. 2013;47(1), 542–548. DOI: 10.1021/es303561n.

[25] Zaniol B, Schiorlin M, Gazza E, Marotta E, Ren XW, Puiatti ME, Rea M, Sonato P, Paradisi C. An emission spectroscopy study of atmospheric plasmas formed by DC and pulsed corona discharges in hydrocarbon contaminated air. Int. J. Plasma Environ. Sci. Technol. 2008;2(1), 65–71. http://www.iesj.org/html/service/ijpest/vol2_no1_2008/IJPEST_Vol2_No1_08_pp65-71.pdf.

[26] Rudolph R, Francke KP, Miessner H. Concentration dependence of VOC decomposition by dielectric barrier discharges. Plasma Chem. Plasma Process. 2002;22(3), 401–412. DOI: 10.1023/A:1015369100161.

[27] Marotta E, Schiorlin M, Rea M, Paradisi C. Products and mechanisms of the oxidation of organic compounds in atmospheric air plasmas. J. Phys. D: Appl. Phys. 2010;43(12), 124011. DOI: 10.1088/0022-3727/43/12/124011.

[28] van Veldhuizen EM., editor. Electrical Discharges for Environmental Purposes: Fundamentals and Applications. New York: Nova Science Publischers; 2000.

[29] Blin-Simiand N, Jorand F, Magne L, Pasquiers S, Postel C, Vacher JR. Plasma reactivity and plasma-surface interactions during treatment of toluene by dielectric barrier discharge. Plasma Chem. Plasma Process. 2008;28(4), 429–466. DOI: 10.1007/s11090-008-9135-1.

[30] Slater RC, Douglas-Hamilton DH. Electron-beam-initiated destruction of low concentrations of vinyl chloride in carrier gases. J. Appl. Phys. 1981;52(9), 5820–5828. DOI: 10.1063/1.329476.

[31] Baulch DL, Cobos CJ, Cox RA, Frank P, Hayman G, Just T, Kerr JA, Murrells T, Pilling MJ, Troe J, Walker RW, Warnatz J. Evaluated kinetic data for combusion modelling. Supplement I. J. Phys. Chem. Ref. Data. 1994;23, 847–1033. http://www.nist.gov/data/PDFfiles/jpcrd484a.pdf.

[32] Bohn B. Formation of Peroxy Radicals from OH−Toluene Adducts and O_2. J. Phys. Chem. A. 2001;105(25), 6092–6101. DOI: 10.1021/jp0033972.

[33] Lias SG. Ionization Energy Evaluation NIST ChemistryWebBook. NIST Standard Reference Database No. 69. Gaithersburg MD: National Institute of Standards and Technology; 2006. http://webbook.nist.gov/chemistry/

[34] Atkinson R, Baulch DL, Cox RA, Crowley JN, Hampson RF, Hynes RG, Jenkin ME, Rossi MJ, Troe J. Evaluated kinetic and photochemical data for atmospheric chemistry: Volume II – gas phase reactions of organic species. Atmos. Chem. Phys. 2006;6, 3625–4055. http://www.atmos-chem-phys.net/6/3625/2006/acp-6-3625-2006.html.

[35] Feng JQ. An analysis of corona currents between two concentric cylindrical electrodes. J. Electrostat. 1999;46(1), 37–48. DOI: 10.1016/S0304-3886(98)00057-6.

[36] Zebboudj Y, Hartmann G. Current and electric field measurements in coaxial system during the positive DC corona in humid air. Eur. Phys. J. Appl. Phys. 1999;7(2), 167–176. DOI: 10.1051/epjap:1999211.

[37] Skalny JD, Mikoviny T, Matejcik S, Mason NJ. An analysis of mass spectrometric study of negative ions extracted from negative corona discharge in air. Int. J. Mass Spectrom. 2004; 233(1-3), 317–324. DOI: 10.1016/j.ijms.2004.01.012.

[38] Sieck LW, Buckley TJ, Herron JT, Green DS. Pulsed Electron-Beam Ionization of Humid Air and Humid Air/Toluene Mixtures: Time-Resolved Cationic Kinetics and

Comparisons with Predictive Models. Plasma Chem. Plasma Process. 2001;21(3), 441–457. DOI: 10.1023/A:1011030627752.

[39] Španěl P, Smith D. Selected ion flow tube studies of the reactions of H_3O^+, NO^+, and O_2^+ with several aromatic and aliphatic hydrocarbons. Int. J. Mass Spectrom. 1998;181(1-3), 1–10. DOI: 10.1016/S1387-3806(98)14114-3.

[40] Arnold ST, Dotan I, Williams S, Viggiano AA, Morris RA. Selected Ion Flow Tube Studies of Air Plasma Cations Reacting with Alkylbenzenes. J. Phys. Chem. A. 2000;104(5), 928–934. DOI: 10.1021/jp9928199.

[41] Baker J, Arey J, Atkinson R. Rate Constants for the Gas-Phase Reactions of OH Radicals with a Series of Hydroxyaldehydes at 296 ± 2 K. J. Phys. Chem. A. 2004;108(34), 7032–7037. DOI: 10.1021/jp048979o.

[42] Seinfeld JH, Pandis SN. Atmospheric Chemistry and Physics: From Air Pollution to Climate Change. Hoboken NJ: John Wiley & Sons, Inc; 2006.

[43] Müller S, Zahn RJ. Air Pollution Control by Non-Thermal Plasma. Contrib. Plasma Phys. 2007;47(7), 520–529. DOI: 10.1002/ctpp.200710067.

[44] Kogelschatz U. Dielectric-Barrier Discharges: Their History, Discharge Physics, and Industrial Applications. Plasma Chem. Plasma Process. 2003;23(1), 1–46. DOI: 10.1023/A:1022470901385.

[45] Manley TC. The Electric Characteristics of the Ozonator Discharge. Trans. Electrochem. Soc. 1943;84(1), 83–96. DOI: 10.1149/1.3071556.

[46] Pate CT, Atkinson R, Pitts JN Jr. The Gas Phase Reaction of O_3 with a Series of Aromatic Hydrocarbons. J. Environ. Sci. Health A. 1976;11(1), 1–10. DOI: 10.1080/10934527609385750.

[47] Vandenbroucke AM, Morent R, De Geyter N, Leys C. Non-thermal plasma for non-catalytic and catalytic VOC abatement. J. Hazard. Mater. 2011;195, 30–54. DOI: 10.1016/j.jhazmat.2011.08.060.

[48] Stamate E, Chen W, Jørgensen L, Jensen TK, Fateev A, Michelsen PK. IR and UV gas absorption measurements during NO_x reduction on an industrial natural gas fired power plant. Fuel. 2010;89(5), 978–985. DOI: 10.1016/j.fuel.2009.11.044.

[49] Kim HH, Ogata A, Futamura S. Oxygen partial pressure-dependent behavior of various catalysts for the total oxidation of VOCs using cycled system of adsorption and oxygen plasma. Appl. Catal. B Environ. 2008;79(4), 356–367. DOI: 10.1016/j.apcatb.2007.10.038.

[50] Rafflenbeul R. Non Thermal Plasma Plants: Experiences from the Industrial Praxis of Air Purification. Presentation at PlasTEP workshop;2010. Available from http://www.plastep.eu/fileadmin/dateien/Downloads/Downloads__Minutes_etc_/100910_Workshop/Vortrag_PPT__INP_Greifswald.pdf

[51] Saulich K, Müller S. Removal of formaldehyde by adsorption and plasma treatment of mineral adsorbent. J. Appl. Phys. D: Appl. Phys. 2013;46(4), 045201. DOI: 10.1088/0022-3727/46/4/045201.

[52] Basner R, Akimalieva A, Brandenburg R. Effect of atmospheric surface plasma on the adsorption of ethanol at activated carbon filter element. Surf. Coat. Tech. 2013;234, 126–134. DOI: 10.1016/j.surfcoat.2012.11.028.

[53] Müller S, Saulich K, Krueger T. Regeneration of Clinoptilolite Loaded with Ammonia by a Non-Thermal Plasma Method. Chem. Ing. Tech. 2012;84(12), 2190–2197. DOI: 10.1002/cite.201200044.

IntechOpen